Analysis of Single Bacterium Dynamics in a Stochastic Model of Toxin-Producing Bacteria

Jamie Paterson[1], Martín López-García[1(✉)], Joseph Gillard[2], Thomas R. Laws[2], Grant Lythe[1], and Carmen Molina-París[1,3]

[1] School of Mathematics, University of Leeds, Leeds, UK
m.lopezgarcia@leeds.ac.uk
[2] CBR Division, Defence Science and Technology Laboratory, Salisbury, UK
[3] T-6 Theoretical Biology and Biophysics, Theoretical Division, Los Alamos National Laboratory, Los Alamos, NM, USA

Abstract. We stochastically model two bacterial populations which can produce toxins. We propose to analyse this biological system by following the dynamics of a single bacterium during its lifetime, as well as its progeny. We study the lifespan of a single bacterium, the number of divisions that this bacterium undergoes, and the number of toxin molecules that it produces during its lifetime. We also compute the mean number of bacteria in the genealogy of the original bacterium and the number of toxin molecules produced by its genealogy. We illustrate the applicability of our methods by considering the bacteria *Bacillus anthracis* and antibiotic treatment, making use of *in vitro* experimental data. We quantify, for the first time, bacterial toxin production by exploiting an *in vitro* assay for the $A16R$ strain, and make use of the resulting parameterised model to illustrate our techniques.

Keywords: Bacteria · Toxins · Stochastic model · Continuous time · Markov chain · Single cell · Antibiotic

1 Introduction

Mathematical modelling has proven to be a robust approach to analyse biological systems of relevance in infection and immunity at different scales, such as the molecular [24], intra-cellular [6], within-host [7] and population (or epidemic) levels [4]. While deterministic models are usually more amenable for mathematical analysis [1], stochastic methods are generally better suited for characterising biological systems involving few individuals [23] or cells [7], or when extinction events play a crucial role [5]. Markov processes, either in discrete or continuous time, have been used in such instances given their mathematical convenience [2]. While non-Markovian dynamics are typically more difficult to analyse [8,14], the Markovian or memoryless property usually allows for mathematical tractability and efficient numerical implementation [12].

P. Ballarini et al. (Eds.): EPEW 2021/ASMTA 2021, LNCS 13104, pp. 210–225, 2021.
https://doi.org/10.1007/978-3-030-91825-5_13

When considering a population of cells in an immune response, or bacteria during an infection, competition for resources is usually represented in terms of logistic growth models [1]. On the other hand, when individuals behave independently (*e.g.,* they do not compete for common resources), the theory of branching processes [18] has been widely applied to follow these populations (of cells or bacteria) over time. Multi-type branching processes [20] allow one to consider different types of bacteria, which might represent different phenotypes [9] or different spatial locations (*e.g.,* tissues or organs) within the body during an infection [7]. The complexity of these processes, and their mathematical tractability, typically depends on the number of compartments considered, and the number of potential events that can occur in the system (*e.g.,* division or death of bacteria, or bacterial movement across compartments) [26].

Novel technological developments have recently allowed for single cells to be precisely followed, together with their progeny [15,17,19,27]. This motivates the idea of mathematically tracking single individuals in these stochastic systems, and to quantify summary statistics related to the lifetime of a single individual (or bacterium in our case), and its progeny or genealogy. Analysing the dynamics of the system by tracking a single individual has already been proposed in related areas such as population dynamics [13] and, more recently, when analysing the stochastic journey of T lymphocytes in lymph nodes and blood [16].

Bacterial systems have been widely studied with stochastic methods in the past [6,7], yet less attention has been paid to the study of toxin-producing bacteria. The production of toxins over time can be especially relevant for certain kinds of bacteria for which the secreted toxins can cause suppression of the host's immune system, and are a key component of pathogenesis *in vivo* [3]. In this work, we illustrate our single cell approach in a stochastic model of two types of toxin-producing bacteria. In particular, we focus on computing the expected lifespan of a single bacterium in this system, as well as the number of toxin molecules secreted and the number of divisions undergone during its lifetime. We also compute two summary statistics that are directly related to the progeny of a single bacterium: the number of bacteria within its genealogy and the number of toxin molecules produced by its genealogy. We illustrate our results by focusing on the bacterium *Bacillus anthracis* and its anthrax toxins. For the *A*16*R B. anthracis* strain we quantify for the first time the rate of protective antigen (PA) production making use of published data from an *in vitro* experimental assay [28]. The resulting parametrized mathematical model serves to illustrate our techniques and allows us to consider antibiotic treatment.

The structure of the manuscript is as follows: in Sect. 2 we introduce the mathematical model. The single bacterium model is discussed in Sect. 3. A number of summary statistics of interest related to a single bacterium and its progeny are analytically studied in Sect. 3. Model calibration for the *A*16*R B. anthracis* strain is carried out in Sect. 4 using data from an *in vitro* experimental assay, and the parameterised model is used in this section to illustrate our methods. Concluding remarks are provided in Sect. 5.

2 The Mathematical Model

Our interest is in modelling a system with two toxin-producing bacterial populations (see Fig. 1). Type-i bacteria, $i \in \{1, 2\}$, can divide with rate λ_i, produce toxins with rate γ_i, die with rate μ_i, or become type-j bacteria, $j \in \{1, 2\}$ $j \neq i$, with rate ν_{ij}. We propose a stochastic model of these events as a continuous time Markov chain (CTMC) $\mathcal{X} = \{(B_1(t), B_2(t), T(t)) : t \geq 0\}$, where $B_i(t)$ denotes the number of type-i bacteria at time $t \geq 0$, $i \in \{1, 2\}$, and $T(t)$ represents the number of toxin molecules at time $t \geq 0$. We assume that bacteria and toxins behave independently of each other, and that toxins are degraded at rate ξ. The space of states of $\mathcal{X}$ is given by $\mathcal{S} = \mathbb{N}_0^3$, where we denote $\mathbb{N}_0 = \mathbb{N} \cup \{0\}$, and the possible one-step transitions between states in $\mathcal{X}$ are depicted in Fig. 1.

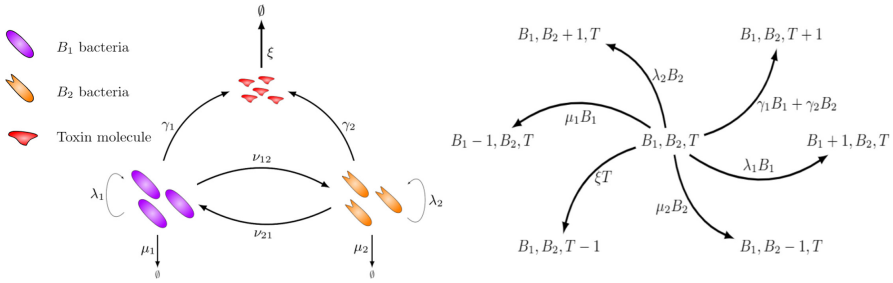

Fig. 1. Left. Diagram showing the dynamics of the two toxin-producing bacterial populations. **Right.** Allowed transitions between states in $\mathcal{X}$ and their rates.

Since each bacterium behaves independently, one can analyse the dynamics of a single bacterium without explicitly modelling the dynamics of the rest of the population. In Sect. 3, we propose a method which allows us to analyse the dynamics of a single bacterium and its progeny. In particular, and by means of first step arguments, we compute the lifespan of a single bacterium, the number of divisions that this bacterium undergoes, and the number of toxin molecules that it produces during its lifetime. We also compute the mean number of cells within the genealogy of the original bacterium and the number of toxin molecules produced by this progeny. We note that a particular advantage of this single bacterium approach is that it can be implemented regardless of the complexity of the model, *i.e.,* regardless of the number of compartments in the model, two compartments in our model (see Fig. 1), or the number of events governing the toxin and bacterial dynamics across compartments, as long as the dynamics of each bacterium is independent of the rest of the population.

3 Dynamics of a Single Bacterium and Its Progeny

Our interest in this section is in following a single bacterium of type i during its lifespan, instead of focusing on the population CTMC $\mathcal{X}$. In particular, we

consider a single bacterium (either of type-1 or type-2) at time $t = 0$, and follow its dynamics during its lifetime by studying the continuous time Markov chain $\mathcal{Y} = \{Y(t) : t > 0\}$, where $Y(t)$ represents the "*state*" of the bacterium at time $t \geq 0$. By state, we mean that the bacterium can be of type-1, type-2 or dead at any given time. Thus, $\mathcal{Y}$ is defined on the state space $S = \{B_1, B_2, \emptyset\}$, where B_i here represents the bacterium being of type-i at any given instant, and $\emptyset$ indicates the bacterium is dead. If the bacterium is of type-i at a given instant, meaning that $\mathcal{Y}$ is in state B_i, production of a toxin molecule does not change its state, and $\mathcal{Y}$ remains in B_i. If a division occurs, we randomly choose one of the daughter cells and consider it to be our bacterium of interest, which remains in state B_i.

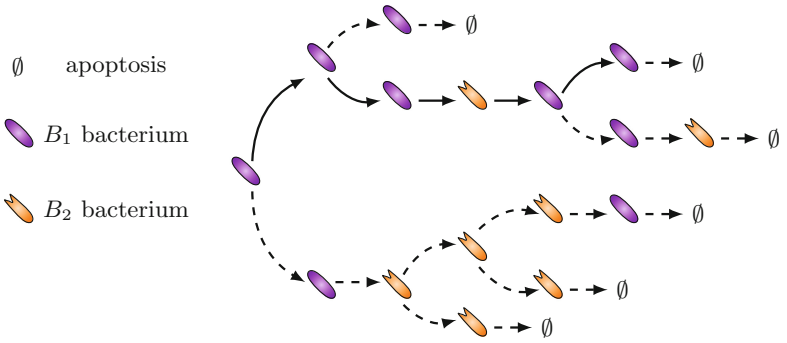

Fig. 2. Example of a stochastic realisation of the population process, starting with one type-1 bacterium. Solid arrows indicate the single bacterium being tracked in process $\mathcal{Y}$. In this realisation, the stochastic process $\mathcal{Y}$ visits states $B_1 \to B_1 \to B_1 \to B_2 \to B_1 \to B_1 \to \emptyset$. Consecutive visits to the same state are due to bacterial division. Toxin production is not explicitly depicted here but can occur during the process.

Figure 2 shows one realisation of the population dynamics for our biological system. The state of the stochastic process $\mathcal{Y}$ only depends on tracking the original bacterium throughout its lifetime, which is depicted via solid arrows. When a division occurs, a daughter is randomly chosen to represent the tracked bacterium of interest. In the following sections we investigate a number of stochastic descriptors or summary statistics that relate to the single bacterium, as well as its genealogy.

3.1 Lifespan of a Bacterium

For an initial bacterium of type i, $i \in \{1, 2\}$, we define its lifespan as the random variable, $T_i = \inf\{t \geq 0 : Y(t) = \emptyset | Y(0) = B_i\}$. We consider the Laplace-Stieltjes transform of T_i given by

$$\phi_i(s) = \mathbb{E}[e^{-sT_i}], \quad \text{Re}(s) \geq 0,$$

which one can compute with first step arguments. This leads to the following equations

$$\phi_1(s) = \frac{\lambda_1}{\Delta_1 + s}\phi_1(s) + \frac{\mu_1}{\Delta_1 + s} + \frac{\gamma_1}{\Delta_1 + s}\phi_1(s) + \frac{\nu_{12}}{\Delta_1 + s}\phi_2(s),$$
$$\phi_2(s) = \frac{\lambda_2}{\Delta_2 + s}\phi_2(s) + \frac{\mu_2}{\Delta_2 + s} + \frac{\gamma_2}{\Delta_2 + s}\phi_2(s) + \frac{\nu_{21}}{\Delta_2 + s}\phi_1(s),$$

with $\Delta_i = \lambda_i + \mu_i + \gamma_i + \nu_{ij}$, $j \in \{1, 2\}$, $j \neq i$. These equations simplify to

$$(\mu_1 + \nu_{12} + s)\,\phi_1(s) = \nu_{12}\phi_2(s) + \mu_1,$$
$$(\mu_2 + \nu_{21} + s)\,\phi_2(s) = \nu_{21}\phi_1(s) + \mu_2.$$

Interestingly, we can see that these equations do not depend on the parameters λ_i (division rate) or γ_i (toxin production rate). This is consistent with our expectations, since division and toxin production events do not affect the lifespan of a bacterium, as can be noticed from inspecting the dynamics in Fig. 1 and Fig. 2. We can find solutions for these equations as follows

$$\phi_1(s) = a^{-1}(s)\frac{1}{\mu_1 + \nu_{12} + s}\left(\frac{\nu_{12}\mu_2}{\mu_2 + \nu_{21} + s} + \mu_1\right),$$
$$\phi_2(s) = a^{-1}(s)\frac{1}{\mu_2 + \nu_{21} + s}\left(\frac{\nu_{21}\mu_1}{\mu_1 + \nu_{12} + s} + \mu_2\right),$$

with $a(s) = 1 - \frac{\nu_{12}\nu_{21}}{(\mu_1+\nu_{12}+s)(\mu_2+\nu_{21}+s)}$. We also note that these expressions would simplify for particular scenarios of the bacterial system. For instance, if the change from type-1 to type-2 bacterium was irreversible so that $\nu_{21} = 0$, one obtains

$$\phi_1(s) = \frac{1}{\mu_1 + \nu_{12} + s}\left(\frac{\nu_{12}\mu_2}{\mu_2 + s} + \mu_1\right),$$
$$\phi_2(s) = \frac{\mu_2}{\mu_2 + s},$$

where we note that in this case $T_2 \sim \text{Exp}(\mu_2)$. This is an interesting and important case to consider since the bacterial conversion with rate ν_{12} and reversion rate $\nu_{21} = 0$ represents the irreversible antibiotic treatment we study and analyse in Sect. 4

One can use the Laplace-Stieltjes transform to compute any order moment of T_i by direct differentiation. For example, the average lifetime of a type-i bacterium is given by

$$\mathbb{E}[T_1] = a^{-1}(0)\frac{1}{\mu_1 + \nu_{12}}\left(\frac{\nu_{12}}{\mu_2 + \nu_{21}} + 1\right),$$
$$\mathbb{E}[T_2] = a^{-1}(0)\frac{1}{\mu_2 + \nu_{21}}\left(\frac{\nu_{21}}{\mu_1 + \nu_{12}} + 1\right).$$

The Laplace-Stieltjes transform allows one to find higher order moments. One such example is the second order moment of the lifespan of a bacterium starting in state 1 when $\nu_{21} = 0$, which is given by

$$\mathbb{E}[T_1^2] = \frac{2}{\mu_1 + \nu_{12}} \left(\frac{1}{\mu_1 + \nu_{12}} + \frac{\nu_{12}}{\mu_2(\mu_1 + \nu_{12})} + \frac{\nu_{12}}{\mu_2^2} \right).$$

3.2 Number of Toxin Molecules Produced by a Bacterium in Its Lifetime

We denote by ω_i the random variable that describes the number of toxin molecules produced by the tracked bacterium during its lifetime, if this bacterium is initially of type i, $i \in \{1, 2\}$. We consider its probability generating function defined as follows

$$\psi_i(z) = \mathbb{E}[z^{\omega_i}],$$

for $|z| \leq 1$. By means of a first step argument, one can show that

$$\begin{aligned}(\mu_1 + \gamma_1(1 - z) + \nu_{12})\psi_1(z) &= \nu_{12}\psi_2(z) + \mu_1,\\ (\mu_2 + \gamma_2(1 - z) + \nu_{21})\psi_2(z) &= \nu_{21}\psi_1(z) + \mu_2.\end{aligned}$$

The equations above have the following solutions

$$\begin{aligned}\psi_1(z) &= b^{-1}(z)\, \frac{1}{\mu_1 + \gamma_1(1 - z) + \nu_{12}} \left(\frac{\nu_{12}\mu_2}{\mu_2 + \nu_{21} + \gamma_2(1 - z)} + \mu_1 \right),\\ \psi_2(z) &= b^{-1}(z)\, \frac{1}{\mu_2 + \gamma_2(1 - z) + \nu_{21}} \left(\frac{\nu_{21}\mu_1}{\mu_1 + \nu_{12} + \gamma_1(1 - z)} + \mu_2 \right),\end{aligned}$$

with $b(z) = 1 - \frac{\nu_{12}\nu_{21}}{(\mu_1 + \gamma_1(1-z) + \nu_{12})(\mu_2 + \gamma_2(1-z) + \nu_{21})}$. Once again, the particular case where $\nu_{21} = 0$ leads to simplified solutions, given by

$$\begin{aligned}\psi_1(z) &= \frac{1}{\mu_1 + \gamma_1(1 - z) + \nu_{12}} \left(\frac{\mu_2}{\mu_2 + \gamma_2(1 - z)}\nu_{12} + \mu_1 \right),\\ \psi_2(z) &= \frac{\mu_2}{\mu_2 + \gamma_2(1 - z)}.\end{aligned}$$

We note that in this case $\omega_2 \sim \text{Geo}(\frac{\mu_2}{\mu_2 + \gamma_2})$. If $\nu_{21} = 0$, it is also possible to obtain the probability mass function of ω_1, which for $n = 0, 1, 2, \ldots$, it can be written as follows

$$\begin{aligned}\mathbb{P}(\omega_1 = n) = \gamma_1^n &\left(\frac{\mu_2}{\gamma_2 + \mu_2}\, \nu_{12} + \mu_1 \right) (\gamma_1 + \nu_{12} + \mu_1)^{-(n+1)}\\ &+ \nu_{12} \frac{\mu_2}{\gamma_2 + \mu_2} \sum_{k=0}^{n-1} \gamma_1^k \left(\frac{\gamma_2}{\gamma_2 + \mu_2} \right)^{n-k} (\gamma_1 + \nu_{12} + \mu_1)^{-(k+1)},\end{aligned}$$

where the sum above is equal to 0 when $n = 0$. The mean number of toxin molecules produced by a single bacterium can be computed from direct differentiation of $\psi_i(z)$ with respect to z. One can show that

$$\mathbb{E}[\omega_1] = b^{-1}(1)\frac{1}{\mu_1 + \nu_{12}}\left(\frac{\gamma_2\nu_{12}}{\mu_2 + \nu_{21}} + \gamma_1\right),$$
$$\mathbb{E}[\omega_2] = b^{-1}(1)\frac{1}{\mu_2 + \nu_{21}}\left(\frac{\gamma_1\nu_{21}}{\mu_1 + \nu_{12}} + \gamma_2\right).$$

3.3 Number of Division Events in the Lifespan of a Bacterium

Let us consider now the number of times that the tracked bacterium divides during its lifetime, D_i, if this bacterium is originally of type i, $i \in \{1, 2\}$. We can define its probability generating function as $\Phi_i(z) = \mathbb{E}[z^{D_i}]$ for $|z| \leq 1$. $\Phi_i(z)$ satisfies the following equations:

$$\Delta_1\Phi_1(z) = \lambda_1 z\Phi_1(z) + \mu_1 + \gamma_1\Phi_1(z) + \nu_{12}\Phi_2(z),$$
$$\Delta_2\Phi_2(z) = \lambda_2 z\Phi_2(z) + \mu_2 + \gamma_2\Phi_2(z) + \nu_{21}\Phi_1(z).$$

These equations have solutions

$$\Phi_1(z) = c^{-1}(z)\frac{1}{\mu_1 + \nu_{12} + \lambda_1(1-z)}\left(\frac{\mu_2\nu_{12}}{\mu_2 + \nu_{21} + \lambda_2(1-z)} + \mu_1\right),$$
$$\Phi_2(z) = c^{-1}(z)\frac{1}{\mu_2 + \nu_{21} + \lambda_2(1-z)}\left(\frac{\mu_1\nu_{21}}{\mu_1 + \nu_{12} + \lambda_1(1-z)} + \mu_2\right),$$

with $c(z) = 1 - \frac{\nu_{12}\nu_{21}}{(\mu_1+\nu_{12}+\lambda_1(1-z))(\mu_2+\nu_{21}+\lambda_2(1-z))}$. We note that these expressions, as one would expect, do not depend on the toxin production rate, γ_i. The desired average number of divisions is then given by

$$\mathbb{E}[D_1] = c^{-1}(1)\frac{1}{\mu_1 + \nu_{12}}\left(\frac{\lambda_2\nu_{12}}{\mu_2 + \nu_{21}} + \lambda_1\right),$$
$$\mathbb{E}[D_2] = c^{-1}(1)\frac{1}{\mu_2 + \nu_{21}}\left(\frac{\lambda_1\nu_{21}}{\mu_1 + \nu_{12}} + \lambda_2\right).$$

Once again, particular scenarios might lead to simplified expressions. If one sets $\nu_{21} = 0$, this yields

$$\mathbb{E}[D_1] = \frac{1}{\mu_1 + \nu_{12}}\left(\frac{\lambda_2\nu_{12}}{\mu_2} + \lambda_1\right),$$
$$\mathbb{E}[D_2] = \frac{\lambda_2}{\mu_2}.$$

This choice implies $D_2 \sim \text{Geo}(\frac{\mu_2}{\mu_2+\lambda_2})$.

3.4 Number of Bacteria in the Genealogy of a Bacterium

We focus now on the random variable describing the number of bacteria in the genealogy of the original bacterium (see Fig. 2). We denote this number as G_i, with i indicating the original bacterium type. We restrict ourselves in what follows to computing the expectation value, $\hat{G}_i = E[G_i]$. If G_i denotes the number of bacteria in the progeny (not including the original bacterium itself, so that $G_1 = 15$ in the particular realization depicted in Fig. 2), then its expectation satisfies

$$\hat{G}_1(\mu_1 + \nu_{12} - \lambda_1) = 2\lambda_1 + \nu_{12}(\hat{G}_2 + 1),$$
$$\hat{G}_2(\mu_2 + \nu_{21} - \lambda_2) = 2\lambda_2 + \nu_{21}(\hat{G}_1 + 1).$$

These quantities will be positive and finite only if $\mu_1+\nu_{12} > \lambda_1$ and $\mu_2+\nu_{21} > \lambda_2$, which become conditions for the number of cells in the genealogy to be finite. Solutions are given by

$$\hat{G}_1 = g^{-1}\frac{1}{\mu_1 + \nu_{12} - \lambda_1}\left(2\lambda_1 + \nu_{12}\frac{\lambda_2 + 2\nu_{21} + \mu_2}{\mu_2 + \nu_{21} - \lambda_2}\right),$$
$$\hat{G}_2 = g^{-1}\frac{1}{\mu_2 + \nu_{21} - \lambda_2}\left(2\lambda_2 + \nu_{21}\frac{\lambda_1 + 2\nu_{12} + \mu_1}{\mu_1 + \nu_{12} - \lambda_1}\right),$$

with $g = 1 - \frac{\nu_{12}\nu_{21}}{(\mu_1+\nu_{12}-\lambda_1)(\mu_2+\nu_{21}-\lambda_2)}$. In order for these averages to be positive, we also require $g > 0$. This leads to a third condition; namely, we have: $\frac{\nu_{21}+\mu_2-\lambda_2}{\nu_{21}} > \frac{\nu_{12}}{\nu_{12}+\mu_1-\lambda_1}$. For the specific case when $\nu_{21} = 0$, one obtains

$$\hat{G}_1 = \frac{1}{\mu_1 + \nu_{12} - \lambda_1}\left(2\lambda_1 + \nu_{12}\frac{\lambda_2 + \mu_2}{\mu_2 - \lambda_2}\right),$$
$$\hat{G}_2 = \frac{2\lambda_2}{\mu_2 - \lambda_2}.$$

3.5 Number of Toxin Molecules Produced by the Genealogy of a Bacterium

Our interest is to mathematically describe a system of toxin-producing bacteria, thus, we now compute the number of toxin molecules produced by the progeny of the original bacterium. We then introduce, Ω_i, the number of toxin molecules produced by the genealogy of an initial type-i bacterium, including any toxins produced by this bacterium. We denote its expectation value by $\hat{\Omega}_i = \mathbb{E}[\Omega_i]$, for $i \in \{1, 2\}$. We note that the number of toxin molecules produced by the genealogy of the single bacterium will be finite if and only if the number of bacteria within the genealogy is finite, so that the conditions on the model parameters described in the previous section are needed in what follows. The expected values, $\hat{\Omega}_1$ and $\hat{\Omega}_2$, satisfy

$$(\mu_1 + \nu_{12} - \lambda_1)\hat{\Omega}_1 = \gamma_1 + \nu_{12}\hat{\Omega}_2,$$
$$(\mu_2 + \nu_{21} - \lambda_2)\hat{\Omega}_2 = \gamma_2 + \nu_{21}\hat{\Omega}_1,$$

with solutions

$$\hat{\Omega}_1 = g^{-1}\frac{1}{\mu_1+\nu_{12}-\lambda_1}\left(\gamma_1+\nu_{12}\frac{\gamma_2}{\mu_2+\nu_{21}-\lambda_2}\right),$$
$$\hat{\Omega}_2 = g^{-1}\frac{1}{\mu_2+\nu_{21}-\lambda_2}\left(\gamma_2+\nu_{21}\frac{\gamma_1}{\mu_1+\nu_{12}-\lambda_1}\right).$$

When $\nu_{21} = 0$ the equations simplify to

$$\hat{\Omega}_1 = \frac{1}{\mu_1+\nu_{12}-\lambda_1}\left(\gamma_1+\nu_{12}\frac{\gamma_2}{\mu_2-\lambda_2}\right),$$
$$\hat{\Omega}_2 = \frac{\gamma_2}{\mu_2-\lambda_2}.$$

We note that there exist links between the expected number of toxin molecules produced by the genealogy and the expected number of bacteria in this genealogy. For instance, when $\nu_{21} = 0$ the average number of bacteria in the genealogy of an original type-2 bacterium, including this original bacterium, is $\hat{G}_2 + 1 = \frac{2\lambda_2}{\mu_2-\lambda_2} + 1 = \frac{\mu_2+\lambda_2}{\mu_2-\lambda_2}$ (see Sect. 3.4). It is clear that, in this case, the genealogy is formed by type-2 bacteria only since $\nu_{21} = 0$. Each of these type-2 bacteria will produce, on average, $\frac{\gamma_2}{\lambda_2+\mu_2}$ toxins (from a geometric distribution) before they decide their fate (division or death). Thus, the mean number of toxin molecules produced by the genealogy is $\frac{\mu_2+\lambda_2}{\mu_2-\lambda_2} \times \frac{\gamma_2}{\lambda_2+\mu_2} = \frac{\gamma_2}{\mu_2-\lambda_2} = \hat{\Omega}_2$, as computed above.

4 Results

We now make use of the previous results to analyse the behaviour of *Bacillus anthracis* bacteria, which causes anthrax infection, in the presence of antibiotic treatment. We consider that non-treated fully vegetative *Bacillus anthracis* bacteria form the B_1 compartment in Fig. 1, while the second compartment, B_2, represents bacteria affected by the antibiotic. *B. anthracis* produces three anthrax exotoxin components [22]: protective antigen (PA), lethal factor (LF) and edema factor (EF). The effectiveness of the anthrax toxins in infecting cells and causing symptoms is mainly due to the protective antigen (PA) capsule [21], with which the other toxin components can form complexes [22]. Therefore, we focus here on the production of PA when implementing our methods. We consider an antibiotic treatment, such as Ciprofloxacin, that inhibits bacterial division and triggers cellular death, so that we shall assume $\mu_2 \geq \mu_1$ and $\lambda_2 = 0$. It is to be expected that the production rate of toxin molecules by antibiotic-treated cells would be at most equal to non-treated cells, and thus, we consider $\gamma_2 \leq \gamma_1$. Bacteria become treated at some rate ν_{12}, and we set $\nu_{21} = 0$ to indicate that the process is irreversible. In Sect. 4.1 we leverage data from an *in vitro* assay for the A16R strain of *B. anthracis* [28] to inform our choice of parameters $(\lambda_1, \mu_1, \gamma_1)$. On the other hand, a global sensitivity analysis of model parameters $(\nu_{12}, \mu_2, \gamma_2)$ allows us in Sect. 4.2 to study the impact of treatment on the summary statistics introduced and analysed in Sect. 3, illustrating the applicability of our techniques.

4.1 Parameter Calibration

In Ref. [28] the authors examine the growth of the A16R *B. anthracis* strain by measuring the viable count of colony forming units (CFU) per mL in the assay for the following time points: $t \in \{4\,\text{h}, 8\,\text{h}, 12\,\text{h}, 16\,\text{h}, 20\,\text{h}\}$. They also develop a sandwich ELISA and cytotoxicity-based method to quantify the concentration of PA every two hours during the experiment, from $t = 4\,\text{h}$ to $t = 26\,\text{h}$. In order to exploit this data set, and to estimate representative values for λ_1, μ_1 and γ_1, we consider its corresponding deterministic model (for the first compartment of non-treated bacteria)

$$\frac{dB}{dt} = (\lambda_1 - \mu_1)B, \quad \frac{dT}{dt} = \gamma_1 B - \xi T,$$

where $B(t)$ is the concentration (in units [CFU/mL]) of bacteria at time t, and $T(t)$ the concentration of PA (in units of [ng/mL]). Results from Ref. [28, Figure 1] support bacterial exponential growth during the first 12 h of the experiment. The bacterial population reaches a carrying capacity after this point, indicating that there exists competition for resources. Thus, since our interest (see Fig. 1) is the analysis of non-competing bacteria, we focus here on the first period of the experiment: $t \in [4\,\text{h}, 12\,\text{h}]$. In particular, we set $\lambda_1 = 0.8\,\text{h}^{-1}$ from Ref. [10], and use bacterial counts from Ref. [28, Figure 1] and toxin concentration measurements from Ref. [28, Figure 4] to estimate the bacterial death rate, μ_1, and the toxin production rate, γ_1. Since the dynamics of the toxin population is likely to be dominated by the production of toxins from an exponentially growing bacterial population, we neglect toxin degradation and set $\xi = 0$ in what follows. We acknowledge that this might lead to underestimating the rate γ_1. Yet, the rate ξ has no effect on any of the summary statistics analysed in Sect. 3.

Parameters μ_1 and γ_1 are estimated making use of the *curve_fit* function from the *scipy.optimize* package in *Python*, which is based on a non-linear least squares method. This leads to point estimates $\mu_1 = 0.43\,\text{h}^{-1}$ and $\gamma_1 = 4.63 \times 10^{-6}$ ng $\text{CFU}^{-1}\text{h}^{-1}$. A comparison between model predictions and observed measurements is provided in Fig. 3. Finally, in order to use our estimate for γ_1 in the stochastic model from Fig. 1, one needs to convert units (from mass in ng to number of molecules). To do this, we note that PA has a relative molecular mass of 83 kD [11,25]. This means that 7.2×10^9 PA molecules have an approximate weight of 1ng, so that $\gamma_1 = 3.34 \times 10^4$ molecules $\text{CFU}^{-1}\text{h}^{-1}$.

4.2 Summary Statistics

We now perform a global sensitivity analysis on a subset of the model parameters for the summary statistics of interest introduced in Sect. 3. We consider the stochastic model of Fig. 1 with baseline parameter values: $\mu_1 = 0.43\ \text{h}^{-1}$, $\lambda_1 = 0.8\ \text{h}^{-1}$ and $\gamma_1 = 3.34 \times 10^4$ molecules $\text{CFU}^{-1}\ \text{h}^{-1}$, according to the calibration carried out in the previous section. To analyse the role of antibiotic treatment (B_1

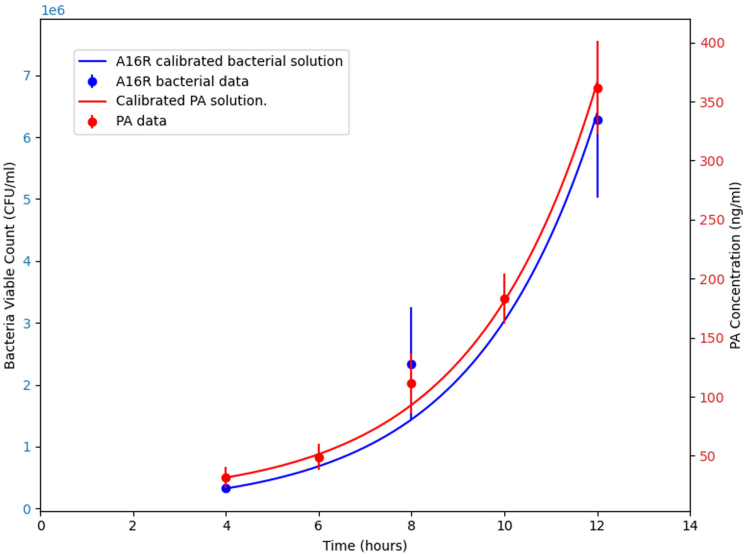

Fig. 3. Mathematical model predictions compared to experimental observations from Ref. [28].

represents non-treated bacteria and B_2 antibiotic-treated bacteria, respectively), we explore parameter regimes with $\nu_{12} > 0$, $\nu_{21} = \lambda_2 = 0$, $\mu_2 \geq \mu_1$ and $\gamma_2 \leq \gamma_1$.

In Fig. 4 we look at summary statistics directly related to the lifetime of a single bacterium. We assume at time $t = 0$ we start with one non-treated bacterium. We first carry out a sensitivity analysis for parameters μ_2, ν_{12} and γ_2. This allows one to analyse the impact of treatment on the tracked bacterium during its lifespan. On the other hand, even when we have a baseline value for μ_1, we vary this parameter when considering the number of divisions undergone by the tracked bacterium, for illustrative purposes. The top-left plot in Fig. 4 shows the impact of treatment on the mean lifespan of the bacterium, $\mathbb{E}[T_1]$, which varies between 1 and 3 h for the parameter values considered. Increasing antibiotic efficiency (in terms of larger values of μ_2 and ν_{12}) leads to shorter lifespans. We note that if one assumes $\mu_2 = \mu_1 = 0.43\ \mathrm{h}^{-1}$, no effect of treatment on the lifespan is expected, and the value of ν_{12} (which is directly related to the rate at which antibiotic can affect bacteria, as well as the concentration of antibiotic present in the system) becomes irrelevant. Finally, increasing values of μ_2 make the value of ν_{12} increasingly relevant, as one would expect.

The top-right plot of Fig. 4 shows the expected number of divisions undergone by the bacterium, $\mathbb{E}[D_1]$, for a range of μ_1 and ν_{12} values. We note here that since $\lambda_2 = 0$, μ_2 has no effect on D_1. Thus, we vary μ_1 instead. As one would expect, increasing values of ν_{12} and μ_1 lead to fewer bacterial divisions. We indicate that in order for the bacterial population to grow as a function of time, each bacterium (on average) needs to undergo more than one division events. We

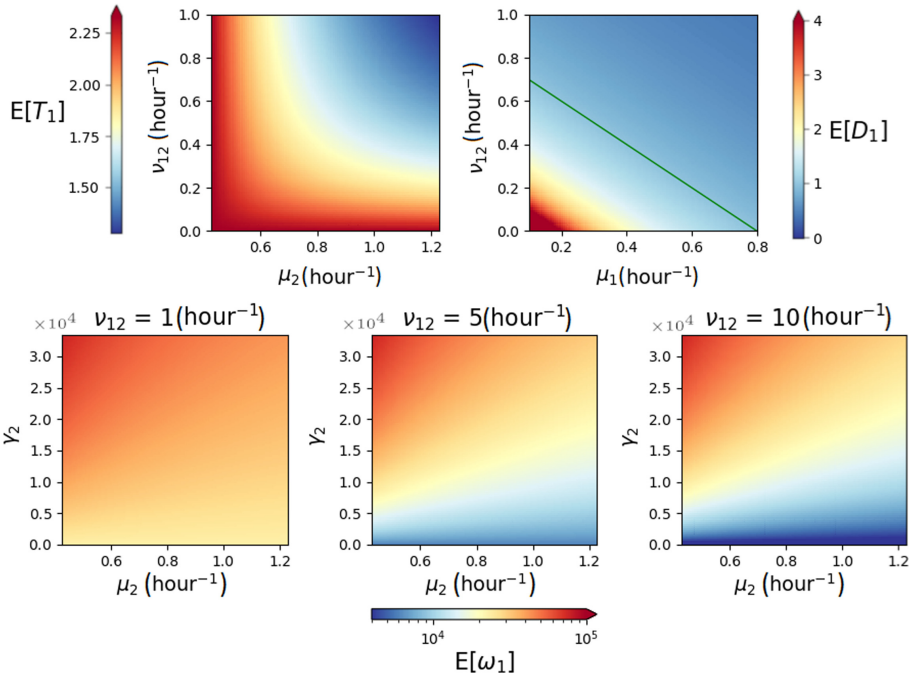

Fig. 4. Top-left. Expected lifespan [*hours*] of a bacterium. **Top-right.** Expected number of divisions during the lifetime of a bacterium. **Bottom.** Expected number of toxin molecules produced by a bacterium during its lifetime for different values of $\nu_{12} \in \{1, 5, 10\}$ (left to right). Units for γ_2 are molecules CFU^{-1} h^{-1}.

highlight the value $\mathbb{E}[D_1] = 1$ by a green line in Fig. 4, which is achieved when $\nu_{12} + \mu_1 = \lambda_1$. The bottom row in Fig. 4 shows the effect of varying ν_{12}, μ_2 and γ_2 on the expected number of toxin molecules produced by a bacterium during its lifetime, $\mathbb{E}[\omega_1]$. Increasing values of μ_2 and ν_{12} can have a significant effect on the number of toxin molecules produced. The values $\gamma_2 = \gamma_1 = 3.34 \times 10^4$ molecules CFU^{-1} h^{-1} and $\mu_2 = \mu_1 = 0.43$ h^{-1} represent no treatment effect for the tracked bacterium, and for these choices the value of ν_{12} has no effect on $\mathbb{E}[\omega_1]$. On the other hand, decreasing values of γ_2 have a significant effect on the predicted number of PA molecules produced, especially for increasing values of ν_{12}.

In Fig. 5 we present summary statistics of relevance to the genealogy of a B_1 bacterium. The top plot of Fig. 5 shows the effect that parameters ν_{12} and μ_1 have on the mean number of cells in the genealogy of a single bacterium, $1 + \hat{G}_1$. We note that, in this plot, the white area corresponds to parameter combinations for which the mean number of cells in the genealogy is not finite. This happens when $\lambda_1 \geq \mu_1 + \nu_{12}$. Values of $\mu_1 + \nu_{12}$ larger but close to λ_1 lead to increasing the mean number of cells in the genealogy, as one would expect. On the other hand, the bottom row of Fig. 5 shows the effect on the number

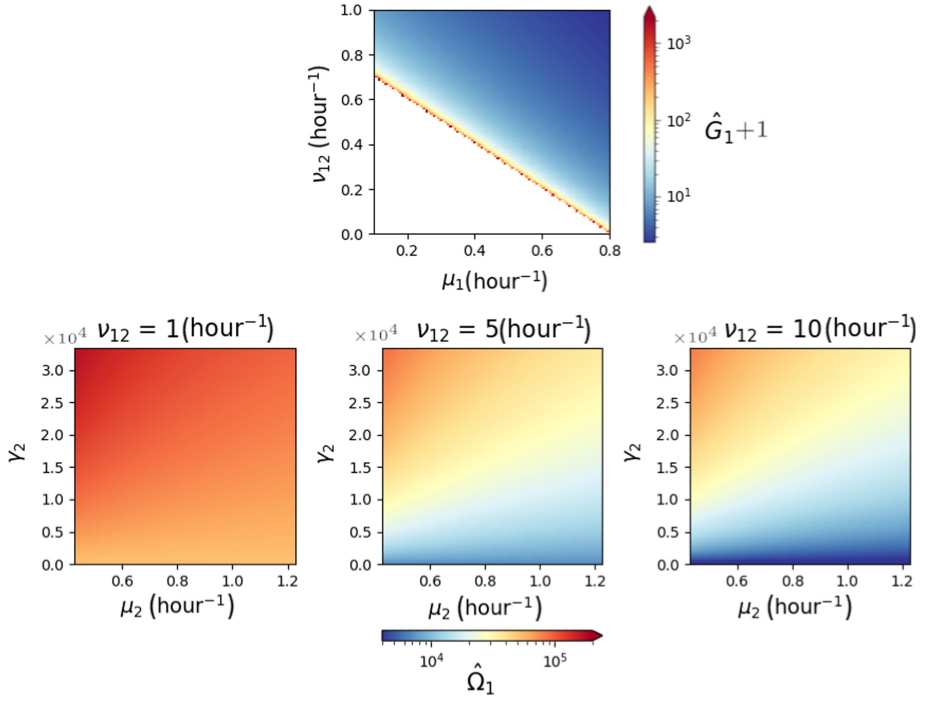

Fig. 5. Top. Mean number of bacteria in the genealogy of a single bacterium. **Bottom.** Mean number of toxin molecules secreted by the genealogy of a single bacterium for different values of $\nu_{12} \in \{1, 5, 10\}$ (from left to right). Units for γ_2 are molecules CFU^{-1} h^{-1}.

of toxin molecules secreted by the genealogy of a single bacterium for varying values of μ_2 and γ_2. We investigate these parameter values for three different choices of $\nu_{12} \in \{1, 5, 10\}$. It is clear that γ_2 has a large impact on the expected value, $\hat{\Omega}_1$, which mimics the similar effect that γ_2 has on its single bacterium counterpart, $\mathbb{E}[\omega_1]$ (see Fig. 4). Figure 4 and Fig. 5 show the significance of ν_{12} on the expected number of toxin molecules produced. Interestingly, as ν_{12} becomes much larger than λ_1, we observe that $\mathbb{E}[\omega_1]$ approaches $\hat{\Omega}_1$, since in this case $1 + \hat{G}_1 \approx 1$ represents the single bacterium of interest.

5 Conclusions

We have defined and analysed a two-compartment stochastic model for toxin-producing bacteria. Our focus has been a number of summary statistics that relate to the lifetime of a single bacterium (tracked over time) and its progeny. In particular, we have studied the lifespan of the bacterium, the number of divisions undergone and the number of toxin molecules produced during its lifetime, as

well as the number of cells in its genealogy, and the number of toxin molecules produced by this progeny. We illustrated in Sect. 4 our methods by focusing on the growth of *B. anthracis* bacteria in the presence of antibiotic treatment. To the best of our knowledge, this is the first approach to quantify the PA production rate in this system. We acknowledge that our estimate for this rate might be an underestimate, given that we neglected PA degradation.

We point out that, although the model considered in Fig. 1 is relatively simple, consisting only of two bacterial compartments, our single bacterium approach can be applied to any network *topology* of compartments, as long as the bacteria behave independently, so that the dynamics of a single bacterium can be effectively followed. Implementing our techniques in more complex systems, such as those representing *in vivo* infection and bacterial dissemination between different organs, remains the aim of future work. We also indicate that, while we have analysed probability generating functions and Laplace-Stieltjes transforms in Sect. 3, we have focused in practice, for simplicity and brevity, on computing the first order moments for the summary statistics of interest. However, this approach can be easily generalised to compute higher order moments or probability mass functions.

Acknowledgements. Jamie Paterson is supported by an EPSRC CASE studentship, project reference 2274495, in partnership with the Defence Science and Technology Laboratory (Dstl). This manuscript has been reviewed at Los Alamos National Laboratory, reference number LA-UR-21-26048.

References

1. Allen, L.J.: An Introduction to Mathematical Biology. Upper Saddle River, Hoboken (2007)
2. Allen, L.J.: An Introduction to Stochastic Processes with Applications to Biology. CRC Press, Boco Raton (2010)
3. Banks, D.J., Barnajian, M., Maldonado-Arocho, F.J., Sanchez, A.M., Bradley, K.A.: Anthrax toxin receptor 2 mediates Bacillus anthracis killing of macrophages following spore challenge. Cell. Microbiol. **7**(8), 1173–1185 (2005)
4. Britton, T.: Stochastic epidemic models: a survey. Math. Biosci. **225**(1), 24–35 (2010)
5. Brockwell, P.J.: The extinction time of a general birth and death process with catastrophes. J. Appl. Probab. **23**, 851–858 (1986)
6. Carruthers, J., López-García, M., Gillard, J.J., Laws, T.R., Lythe, G., Molina-París, C.: A novel stochastic multi-scale model of Francisella tularensis infection to predict risk of infection in a laboratory. Front. Microbiol. **9**, 1165 (2018)
7. Carruthers, J., et al.: Stochastic dynamics of Francisella tularensis infection and replication. PLoS Comput. Biol. **16**(6), e1007752 (2020)
8. Castro, M., López-García, M., Lythe, G., Molina-París, C.: First passage events in biological systems with non-exponential inter-event times. Sci. Rep. **8**(1), 1–16 (2018)
9. Choi, P.J., Cai, L., Frieda, K., Xie, X.S.: A stochastic single-molecule event triggers phenotype switching of a bacterial cell. Science **322**(5900), 442–446 (2008)

10. Day, J., Friedman, A., Schlesinger, L.S.: Modeling the host response to inhalation anthrax. J. Theor. Biol. **276**(1), 199–208 (2011)
11. Fabre, L., et al.: Structure of anthrax lethal toxin prepare complex suggests a pathway for efficient cell entry. J. Gen. Physiol. **148**(4), 313–324 (2016)
12. Gillespie, D.T.: Exact stochastic simulation of coupled chemical reactions. J. Phys. Chem. **81**(25), 2340–2361 (1977)
13. Gómez-Corral, A., López-García, M.: Lifetime and reproduction of a marked individual in a two-species competition process. Appl. Math. Comput. **264**, 223–245 (2015)
14. Gómez-Corral, A., López-García, M.: On SIR epidemic models with generally distributed infectious periods: number of secondary cases and probability of infection. Int. J. Biomath. **10**(02), 1750024 (2017)
15. Herzenberg, L.A., Parks, D., Sahaf, B., Perez, O., Roederer, M., Herzenberg, L.A.: The history and future of the fluorescence activated cell sorter and flow cytometry: a view from Stanford. Clin. Chem. **48**(10), 1819–1827 (2002)
16. de la Higuera, L., López-García, M., Castro, M., Abourashchi, N., Lythe, G., Molina-París, C.: Fate of a naive T cell: a stochastic journey. Front. Immunol. **10**, 194 (2019)
17. Johnson, J., Nowicki, M.O., Lee, C.H., Chiocca, E.A., Viapiano, M.S., Lawler, S.E., Lannutti, J.J.: Quantitative analysis of complex glioma cell migration on electrospun polycaprolactone using time-lapse microscopy. Tissue Eng. Part C Methods **15**(4), 531–540 (2009)
18. Kimmel, M., Axelrod, D.E.: Branching Processes in Biology (2002)
19. Krutzik, P.O., Nolan, G.P.: Fluorescent cell barcoding in flow cytometry allows high-throughput drug screening and signaling profiling. Nat. Methods **3**(5), 361–368 (2006)
20. Kyprianou, A.E., Palau, S.: Extinction properties of multi-type continuous-state branching processes. Stochast. Processes Appl. **128**(10), 3466–3489 (2018)
21. Leppla, S.H.: Anthrax toxin. In: Aktories, K., Just, I. (eds.) Bacterial Protein Toxins. HEP, vol. 145, pp. 445–472. Springer, Heidelberg (2000). https://doi.org/10.1007/978-3-662-05971-5_19
22. Liu, S., Moayeri, M., Leppla, S.H.: Anthrax lethal and edema toxins in anthrax pathogenesis. Trends Microbiol. **22**(6), 317–325 (2014)
23. López-García, M.: Stochastic descriptors in an SIR epidemic model for heterogeneous individuals in small networks. Math. Biosci. **271**, 42–61 (2016)
24. López-García, M., Nowicka, M., Bendtsen, C., Lythe, G., Ponnambalam, S., Molina-París, C.: Quantifying the phosphorylation timescales of receptor-ligand complexes: a Markovian matrix-analytic approach. Open Biol. **8**(9), 180126 (2018)
25. Petosa, C., Collier, R.J., Klimpel, K.R., Leppla, S.H., Liddington, R.C.: Crystal structure of the anthrax toxin protective antigen. Nature **385**(6619), 833–838 (1997)
26. Thakur, A., Rescigno, A., Schafer, D.: On the stochastic theory of compartments: II. Multi-compartment systems. Bull. Math. Biol. **35**(1), 263–271 (1973)
27. Westera, L., et al.: Closing the gap between T-cell life span estimates from stable isotope-labeling studies in mice and humans. Blood J. Am. Soc. Hematol. **122**(13), 2205–2212 (2013)
28. Zai, X., et al.: Quantitative determination of lethal toxin proteins in culture supernatant of human live anthrax vaccine bacillus anthracis A16R. Toxins **8**(3), 56 (2016)